Vol. 74: 145–160, 2017
https://doi.org/10.3354/cr01493

CLIMATE RESEARCH
Clim Res

Published December 27

Relating warm season hydroclimatic variability in the southern Appalachians to synoptic weather patterns using self-organizing maps

Johnathan W. Sugg[1,*], Charles E. Konrad II[2]

[1]Department of Geography and Planning, Appalachian State University, Boone, North Carolina 28608, USA
[2]Department of Geography, University of North Carolina at Chapel Hill, Chapel Hill, North Carolina 27599, USA

ABSTRACT: Hydroclimatic variability has increased in recent decades across the southeastern US, with more frequent droughts and heavy precipitation events. Among these extremes, past research reveals that there is much variety in the synoptic-scale circulation that controls warm-season precipitation. However, research has yet to examine the subtle variation between these circulation patterns and their influence on hydroclimate variability. This is particularly the case in the southern Appalachian Mountains, where topographic complexity mediates the relationship between large-scale circulation and precipitation characteristics. In this study, we use a self-organizing map to classify and spatially visualize synoptic-scale circulation patterns over the southeastern US from 1979 to 2014. The patterns identified in the self-organizing map are linked with daily precipitation characteristics in the region. Our results demonstrate that underlying topographic features have a marked influence on the hydroclimate, and this influence varies according to the configuration of circulation. Greater frequencies of light precipitation are observed across broad-scale regions of high elevation, to varying degrees, no matter which circulation pattern is present. In contrast, precipitation frequencies along interior valleys and leeward slopes are lower and largely limited to a subset of circulation patterns. This study demonstrates how shifts in the large-scale circulation are likely to alter the occurrence of different types of warm-season precipitation events across mountain catchments.

KEY WORDS: Hydroclimatic variability · Self-organizing maps · Southern Appalachian Mountains

1. INTRODUCTION

Mountains are the water towers of the world, supplying a large proportion of freshwater resources to surrounding lowland regions (Messerli et al. 2004, Viviroli et al. 2007). However, the hydroclimatology of mountain regions remains poorly understood, particularly in the context of climate variability and change (de Jong et al. 2009). Observations indicate that drought and heavy precipitation have increased throughout some mid-latitude regions during the last century (Hartmann et al. 2013) and future projections show a continuation of these trends to varying degrees (Christensen et al. 2013). Although research has linked increased hydroclimatic variability with changes in atmospheric circulation (Li et al. 2011, Diem 2013), our understanding of the synoptic patterns and their influence on precipitation events in mountain regions remains limited. Identifying the primary circulation patterns that are associated with different types of precipitation events, and revealing how these vary across the complex terrain in mountain regions, is therefore a vital component to improve future model projections and provide process-based evaluations of their performance.

The purpose of this paper is to understand how large-scale circulation patterns control the occurrence of precipitation across widely varying topographic settings. We focus on the southern Appalachian Mountains (SAM), a mid-latitude mountain

*Corresponding author: suggjw@appstate.edu

region located in the southeastern US (SEUS), which contains much hydroclimatic and topographic variability.

1.1. Synoptic-scale circulation controls on precipitation in mountains

Synoptic-scale circulation features exert a strong control on daily precipitation by affecting the stability of the lower tropospheric air column and directing moisture transport across the SEUS. The most important feature during the warm season is the North Atlantic Subtropical High (NASH), a broad-scale ridge of high pressure centered off the east coast of North America (Kam et al. 2014). Though the NASH is a semi-permanent feature from the surface through the middle troposphere, its orientation and movement influences the positioning of large-scale ridge and trough patterns in the middle troposphere across North America (Wang et al. 2010, Li et al. 2011). When the NASH is displaced to the northwest of its climatological position, middle tropospheric ridging is present across the SAM, resulting in below-normal precipitation amounts (Diem 2013). Likewise, displacement of the NASH to the southeast of its climatological position is tied to the occurrence of troughing and above-normal precipitation amounts. The duration of hydroclimatic regimes is also related to the persistence of features, as a stationary pattern of ridging results in persistent dry periods, while a stationary pattern of troughing results in persistent wet periods (Diem 2006).

Synoptic-scale circulation features also influence the spatial pattern of precipitation. During the warm season, a moist atmosphere supports the development of showers and thundershowers on many days (Maddox et al. 1979), especially during the afternoon and early evening. However, the direction of low-level circulation and the positioning of features in the middle troposphere dictate the extent of rainfall over an area. In some cases, thunderstorms are organized into mesoscale convective systems (Doswell et al. 1996) that often weaken as they approach and cross portions of the SAM. These systems can occur immediately downstream (i.e. east) of a middle tropospheric short wave trough, and in the region of northwesterly flow between a large upstream ridge and downstream trough (Konrad 1997). In addition, spatial patterns of precipitation are mediated by the geometry and orientation of features in the local-scale topography (Lin et al. 2001).

1.2. Spatiotemporal patterns of precipitation

Precipitation in mountain regions is characterized by much spatial variability. Most studies of orographic precipitation have utilized a relatively small number of precipitation gauges. While they can provide statistically robust assessments at broad spatial scales, station networks are plagued by coarse spatial representation, especially in areas of topographic complexity. The majority of rain gauges are located in valleys or low-lying areas, and high elevations are typically undersampled (Barry 2008), meaning that the hydroclimatic regime in many mountain regions remains poorly understood. The few studies that benefit from a dense network of rain gauges (e.g. Prat & Barros 2010) are often confined to local scales, limiting the ability to extrapolate results over a broader region. Regression-based studies seek to overcome these limitations by incorporating geographic and topographic parameters to predict precipitation on varying slope aspects and elevations (Basist et al. 1994, Konrad 1996), but are also subject to the limitation of station locations. Until recently, spatially gridded and continuous precipitation fields based on modeling approaches were unavailable. Multi-sensor precipitation estimation and PRISM model analyses drastically improved the daily representation of rainfall in mountainous terrain, especially at local scales (Daly et al. 1994, Zhang et al. 2011).

Precipitation in mountain regions is also characterized by much temporal variability. The hydroclimate regime across the SEUS is changing, with longer and more frequent dry periods found along with an increase in heavy precipitation events (Labosier & Quiring 2013). Several studies support this finding. Li et al. (2011) found that summer rainfall variability increased over the last 30 yr. Specifically, the frequency of light (0.1–1 mm d^{-1}) and medium (1–10 mm d^{-1}) rainfall events decreased and coincided with an increase in the frequency of heavy rainfall events (>10 mm d^{-1}) (Wang et al. 2010). Recent research suggests that the increased rainfall variability is directly influenced by both variations in atmospheric humidity (Diem 2013), and changes in the location and movement of primary circulation components, including the NASH, over the SEUS (Li et al. 2012).

Hydroclimatic extremes and their impacts pose risks for ecosystems and populations in the SAM. The region serves as a valuable water tower for the SEUS, and its headwater catchments supply freshwater to several of the most rapidly growing metropolitan areas, including Atlanta, Georgia, Charlotte, North Carolina, and Knoxville, Tennessee (Kramer & Eisen-

Hecht 2002, Ruhl 2005). Additionally, heavy rainfall in mountain regions increases stormflow runoff and flooding, especially in portions of the region where surface mining and reclamation result in deforestation and soil compaction (Negley & Eshleman 2006). The hydroclimate also regulates valuable ecosystem services. The SAM is home to ecosystems that house a variety of biologically diverse and endemic species. Endangered red spruce–Fraser fir species in mountain cloud forests (Reinhardt & Smith 2008) and *Plethodon* salamanders (Caruso et al. 2014) are 2 examples of taxa that are particularly vulnerable to future hydroclimatic changes.

Although much research addresses the broad hydroclimatic trends across the SEUS, precipitation variability in the SAM is still poorly understood at daily time scales. The vagaries of wind direction and its influence on the daily precipitation patterns remain unexamined in the SAM. In addition, research has failed to address how the spatial patterns of daily precipitation are manifested under the recent trend towards increased hydroclimate extremes. The following research questions were used to guide this study: (1) which synoptic patterns are tied to different precipitation events in the SAM during the warm season; and (2) among the identified patterns, what is the spatial distribution of precipitation events across the different physiographic regions of the SAM?

2. MATERIALS AND METHODS

2.1. Study area — Southern Appalachian Mountains

The SAM region is a mid-latitude mountain environment in the SEUS with much hydroclimatic variability and topographic complexity. Although the warm season, lower-tropospheric circulation prevails from the southwest, it displays much day-to-day variability (e.g. from northwesterly to southeasterly) (Konrad 1997, Diem 2006). The northwest portion of the SAM is generally wetter under northwesterly low-level flow due to orographic lifting. In the southeast portion of the SAM, southerly to easterly low-level flow encourages precipitation through orographic lifting or orographically mediated convection (Parker & Ahijevych 2007, Rickenbach et al. 2015). The direction of low-level flow thus influences whether topographic features are exposed to moisture advection from the Atlantic Ocean and Gulf of Mexico or rain-shadowed (Konrad 1996).

Fig. 1 shows the 9 physiographic regions of the SAM and the mean summer precipitation, derived from PRISM precipitation estimates (2002–2014). (1) The northwest slopes and plateau region (Table 1), which includes the Allegheny and Cumberland Plateaus, are located along the northwestern boundary of the SAM. Although the region is generally rain-shadowed from the typical moisture transport

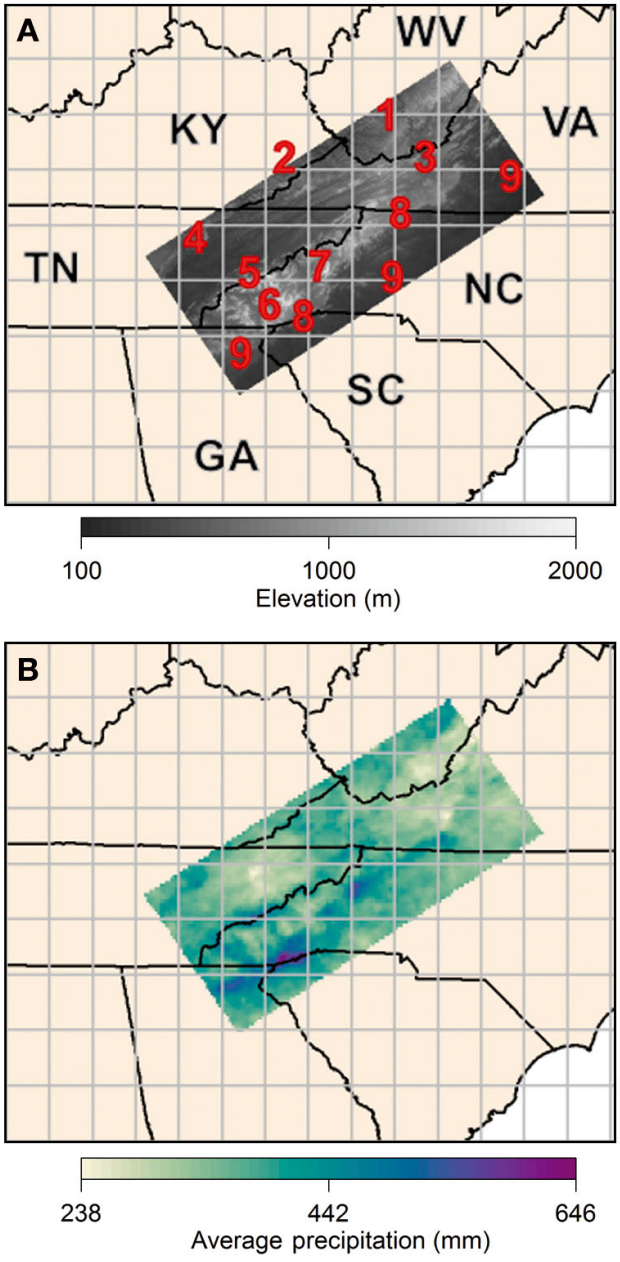

Fig. 1. Study area map of the southern Appalachian Mountain (SAM) region depicting (A) elevation and (B) average summer precipitation, derived from PRISM (2002–2014). Important physiographic features across the SAM are also highlighted, including (1) the Allegheny and (2) Cumberland Plateaus, (3) New River Valley, (4) Tennessee Valley, (5) Great Smoky Mountains, (6) Balsam Range, (7) Black Mountains, (8) Blue Ridge Escarpment, and (9) Piedmont

Table 1. Physiographic features in the southern Appalachian Mountains (SAM) are referred to according to a general reference name. The physiographic features are grouped according to their index number, identified in Fig. 1

Index number	Physiographic feature(s)	General reference name
1, 2	Allegheny Plateau, Cumberland Plateau	Northwest slopes and plateau
3, 4	New River Valley, Tennessee Valley	Intervening valleys
5, 6, 7	Great Smoky Mountains, Balsam Range, Black Mountains	Interior highlands
8	Blue Ridge Escarpment	Blue Ridge and foothills
9	North Carolina–Virginia Piedmont	Piedmont

from the south and east, average summer precipitation is roughly 400 mm. Konrad (2001) documented a lower frequency of heavy rainfall events occurring in this region (index numbers 1 and 2). (2) The intervening valley region, which includes the New River and Tennessee Valleys (index numbers 3 and 4), is located farther towards the southeast and runs along the interior of the SAM. The intervening valleys are rain-shadowed and thus blocked from moisture advection in nearly every direction. As a result, some portions receive less than 254 mm of precipitation while the adjacent ridgelines receive 400 mm. (3) The most topographically complex area is the interior highlands region, which includes the Great Smoky Mountains, Balsam Range, and Black Mountains (index numbers 5, 6, and 7). This region receives a greater amount of precipitation (>500 mm) as a result of the elevation and topographic exposure. However, it is also intersected by several major river valleys, where seasonal precipitation totals are as low as 300 mm. (4) The Blue Ridge and foothills region includes the Blue Ridge Escarpment (index number 8), which is highly exposed to very moist southerly flow. As a result, it is the wettest region in the interior SEUS (>600 mm) during the summer. (5) The Piedmont region (index number 9) is located southeast of the escarpment along the southeastern boundary of the SAM. Precipitation in this region is 300 mm on average per season.

2.2. DATA

Daily 500 hPa geopotential height (GPH) and mean sea level pressure (MSLP) data are extracted from the European Centre for Medium-Range Weather Forecasts (ECMWF) ERA-Interim reanalysis (Dee et al. 2011). ERA-Interim is a global atmospheric reanalysis available from 1979 to present, which resolves atmospheric and surface variables at ~80 km resolution across 60 vertical levels (Berrisford et al. 2009). The reanalysis fields provide a multivariate, spatially complete, and coherent record of atmospheric circulation (Dee et al. 2011). Reanalysis datasets have drastically improved due to the increased quality of observational input data, and while they do not represent actual observations, they provide the most accurate representation of historical states of atmospheric variables (Dee et al. 2011).

In this study, synoptic features in the lower and middle tropospheric circulation across the SEUS are identified and related to patterns of precipitation. 500 hPa GPH and MSLP data were downloaded across a quadrangle from 27.3° N to 40.8° N in latitude and 91° W to 72° W in longitude. The spatial domain includes much of eastern North America, as well as portions of the Gulf of Mexico and the western Atlantic Ocean (Fig. 1). Data were obtained at 6 h intervals and averaged every 24 h period for the months June, July, and August over the period 1979–2014.

Daily precipitation data from PRISM are used to identify hydroclimatic patterns in the SAM (Prism Climate Group 2015). The PRISM interpolation method provides a spatially continuous, gridded raster surface at 4 × 4 km resolution over the US. For each PRISM day, observations from surface stations are weighted in a regression model according to the regional physiographic characteristics that influence precipitation development. Multi-sensor precipitation estimates (MPE) are also used in PRISM to refine precipitation variations at finer scales (Daly et al. 2008). Although PRISM provides a useful model for studies in mountainous terrain, we recognize that each grid cell provides an average aerial estimate of precipitation. Daily data were collected for this study from 2002 to 2014 for the months of June, July, and August.

2.3. IMPLEMENTATION OF THE SELF-ORGANIZING MAP

In this study, atmospheric circulation patterns are classified using a form of artificial neural network,

called a self-organizing map (SOM). SOMs may be used to explore the relationships between surface climate variables and atmospheric circulation, and there are numerous examples with various applications in recent years (Lynch et al. 2006, Wise & Dannenberg 2014, Gibson et al. 2016a). The SOM is used in a similar manner to other synoptic classification methods including manual or automated approaches, though the resulting classes are actually theoretical patterns representing the data distribution and not composites of the actual data. These classes are represented in a 2-dimensional array of nodes that self-organizes through an iterative training process (Sheridan & Lee 2011).

Daily atmospheric circulation patterns are classified over the SEUS from 1979 to 2014 using a 3 × 4 SOM with 12 nodes. Since the number of nodes influences the variability of patterns in the array (Gibson et al. 2016b), a 4 × 4 and a 4 × 5 SOM with 16 and 20 nodes, respectively, are also trained to compare the distribution of circulation patterns in different-sized arrays (not shown). Horton et al. (2015) conducted a similar analysis of extreme temperature patterns using SOMs and determined the sensitivity of their results to the number of nodes. Although the larger-sized SOMs increase the number of circulation categories in the array, they reduce the amount of change in the patterns from node to node. Circulation patterns belonging to the same neighborhood of nodes in the array are often indistinguishable, which limits the ability to draw conclusions about the variability between circulation patterns. The 3 × 4 SOM with 12 nodes, in contrast, increases variability between the nodes and retains visually interpretable differences in the circulation from node to node. Based on the sensitivity tests, this study utilizes the 12-node configuration of the SOM.

To emphasize patterns in the middle troposphere, the SOM is trained using daily ERA-Interim 500 mb GPH data over 36 summer seasons. The patterns aggregated in the SOM space thus represent 3312 circulation days over the SEUS. MSLP fields are then composited by taking an average of the days assigned to each node in order to study the low level flow. We determine the primary direction of the moisture flux and integrated vertical transport in each node by compositing the 500 and 850 mb U and V components of the wind. The most frequently occurring winds over the SAM are then displayed by their magnitude and direction in the SOM. Two metrics are calculated to assess the temporal character of the circulation in each node. (1) The frequency of each circulation pattern is computed as the percentage of time that the identified pattern is present during the summer. (2) To compare the duration of nodes, we also calculate the persistence of each circulation pattern. The persistence values are presented as a ratio that is determined by the number of times a pattern's duration is ≥2 d divided by the total number of times the pattern's duration is 1 d. The frequency metric is commonly applied in synoptic climatology, yet it alone cannot provide a thorough framework to evaluate the temporal attributes of circulation patterns. The persistence metric thus provides a powerful addition to evaluate the influence of synoptic-scale circulation on precipitation (Gibson et al. 2016b)

In this study we employ a sequential training scheme for the SOM. Circulation patterns are selected from the data space through random initialization and placed onto a network of nodes with rectangular topology (Kohonen 1997, Wehrens & Buydens 2007). Each node is then assigned a reference vector coefficient and the remaining daily circulation patterns, or input vectors, are sequentially presented to the map. In this study, the input vectors are presented to the network 100 times, and the learning rate vector declines linearly from 0.05 to 0.01 over the course of the iterations. Each node and the adjacent neighborhood of nodes is updated to reflect the best matching units, which are closest in the data space, allowing the map to self-organize until the final arrangement of circulation patterns is present. A 67% training radius is used across the network to define the area of nodes that are updated with each iteration. The radius parameter is roughly equivalent to two-thirds of the array, with a starting point of 2 and an ending point of 0. The sum of squares formula is used as the distance decay function.

The SOM trains until there are no more changes in node locations within the array (Hewitson & Crane 2002). At this stagnation threshold, the nodes in the array provide a theoretical representation of atmospheric circulation, which can then be related to the different types of precipitation events. Individual circulation patterns from the original data may therefore contribute to the pattern that is present in one or more nodes. The nodes are not discrete, but rather comprised of all possible circulation patterns that exhibit similarity to the specific node in that area of the SOM space. For further discussion of the various implementations of the SOM in synoptic climatology, we refer the reader to Hewitson & Crane (2002), Sheridan & Lee (2011), and Skific & Francis (2012).

There are 2 major benefits of the SOM over traditional types of synoptic classification. (1) The SOM

is more versatile. No assumptions about the data have to be made in advance to run the classifications (Yarnal et al. 2001). (2) The SOM is a spatially organized visualization tool that allows the user to see commonalities and differences among circulation patterns. This feature increases the ability to distinguish variations in the circulation pattern from node to node, and provides a spatial organization that is absent in other techniques. Synoptic regimes that are very different from each other tend to be far apart in the array, and regimes that exhibit much similarity tend to be located adjacent to one another. While these theoretical patterns may only closely resemble a few of the patterns in the observations, they provide a reasonable representation of the entire distribution (Hewitson & Crane 2002). In contrast, the reduction in dimensionality can also be a limitation. The interpretation of the SOM must be done with caution because extreme events may be tied to infrequent patterns that are not represented in a SOM node (Huva et al. 2015).

2.4. Circulation connections with precipitation

Daily PRISM data are used to describe the summer season frequencies of different types of precipitation events across the SAM. Precipitation events are divided into the following bins, which reflect the amounts of precipitation that are received over a 24 h period: none (<0.25 mm), very light (0.25–2.53 mm), light (2.54–12.69 mm), moderate (12.70–38.0 mm), and heavy (≥38.1 mm). These thresholds were derived from sensitivity tests, and they characterize the common spatiotemporal patterns of each precipitation event type. This is especially true of light rainfall, which is the main freshwater supply in many mountain regions, as it exhibits a high frequency of occurrence across ridgelines and areas of mean high elevation (Bhatt & Nakamura 2005, Yang & Gong 2010, Bruijnzeel et al. 2011, Wilson & Barros 2014).

The character of the daily precipitation regime is determined based on the following steps. (1) Each day of the study period is assigned to the SOM node that corresponds most closely with the 500 mb circulation pattern. (2) We calculate the mean precipitation associated with each node. (3) The frequency of each precipitation event type is linked with the circulation patterns in the SOM by calculating the percentage of days in which each precipitation event type occurs over each grid cell in the SAM.

3. RESULTS

3.1. Classification of the synoptic-scale circulation

To reference patterns within the SOM, in Fig. 2 the rows are labeled 1–3 from top to bottom and the columns are labeled A–D from left to right. Node locations are specified using their row and column combination, or simply by groups of patterns according to row or column. There is a wide range of circulation patterns identified across the SOM over the SEUS during the study period (Fig. 2). In general, middle tropospheric troughs are positioned upstream or over the SAM along the left side of the SOM (i.e. columns A and B) and ridging patterns are located over or upstream of the SAM along the right side of the SOM (i.e. columns C and D). The corresponding composite surface patterns feature a surface wave and trailing front, with low pressure across the SAM (columns A and B) and high pressure across the domain in association with the northwest ridge of the NASH (columns C and D).

We summarize the middle tropospheric circulation and corresponding surface pressure patterns in a clockwise fashion around the SOM. The row 3 maps reveal variations in the positioning of a ridge from overhead in D3 to downstream in A3. The corresponding MSLP composites depict a strong NASH centered immediately east of the region in D3 to a much weaker NASH situated far off the coast in A3, along with the approach of a surface front from the northwest. The map patterns in the third row are present on roughly 45% of the days during the summer, with node B3 occurring the most frequently. The map pattern in D3 is also the second most persistent type of circulation across the SOM, and 56% of the events occurred with a node duration of ≥2 d. Column A exhibits troughing across the region that is increasingly pronounced from nodes A3 to A1. The trough is situated slightly upstream in nodes A3 and A2 and slightly downstream in A1. All 3 of these 500 mb patterns correspond with the approach (A3) and passage (A2–A1) of a surface front and trough, as revealed in the MSLP composites. While their frequency of occurrence during the study period decreases from nodes A3 to A1, the persistence of these nodes increases. In fact, node A1 occurs less frequently (2.6% of days) than any other node, which highlights the infrequent occurrence of marked troughing across the region during the summer time. However, it is the most persistent type of circulation across the SOM, with 60% of the events occurring with a node duration of ≥2 d, indi-

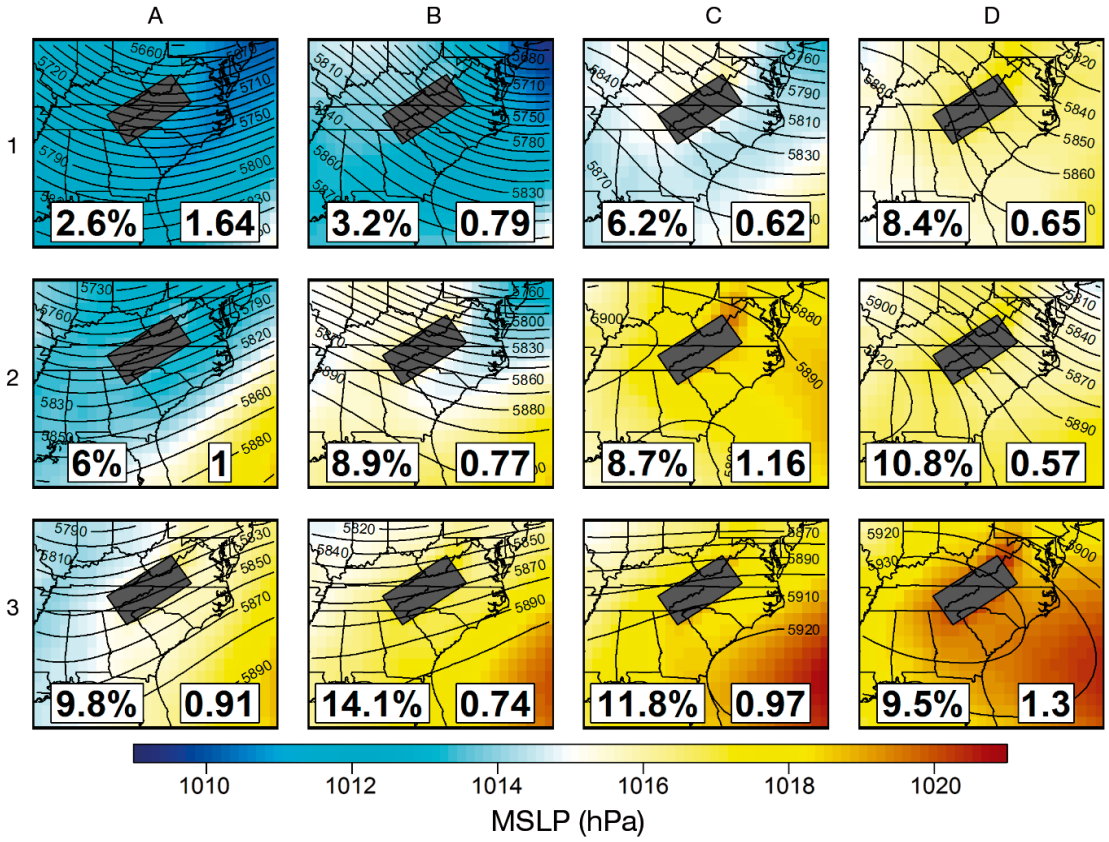

Fig. 2. Self-organizing map trained from ERA-Interim daily 500 mb geopotential height (GPH) fields (contours) for the warm season during the period 1979–2014. The GPH contour interval is 10 m for each node. The composited mean sea level pressure (MSLP) is composited based on the days assigned to each node. The frequency (left) and duration (right) of each pattern is also given in each node

cating the relatively slow-moving nature of these troughs during the summer time.

The map patterns in row 1 depict a trough that is present overhead in A1 to downstream of the region in B1 and C1. The trough is most pronounced in nodes A1 and B1 and much weaker in nodes C1 and D1. Nodes C1 and D1 also exhibit an upstream ridge immediately west of the SAM, which is most developed in node D1. At the surface, the corresponding patterns in nodes A1 and B1 depict a front or surface trough exiting the region and a high pressure filling in to the west behind the trough in nodes C1 and D1. There is a marked increase in the frequency of the circulation patterns from C1 (2.6%) to D1 (8.4%), and a marked decrease in their persistence. In fact, nodes C1 and D1 exhibit the second and third lowest duration of any circulation pattern in the SOM, with 37–38% of the events occurring with a node duration of ≥2 d. Column D exhibits a pattern of increased ridging from upstream of the region (D1) to overhead of the region in (D3). This increase in ridging corresponds with an increase in the strength of the NASH and positioning closer to the SAM in the surface pressure composites. Node D2 exhibits a relatively high frequency of occurrence (10.8%), yet it is the least persistent circulation pattern across the SOM, as only 35% of the events occurred with a node duration of ≥2 d.

3.2. The hydroclimate of the SAM and its relationship with circulation patterns

The frequency of each of the precipitation event types across the SAM is presented in Fig. 3. Dry days with no precipitation are the most frequent during the summer, occurring >50% of the time across the majority of the SAM and up to 65% of the time in the intervening valleys and Piedmont. Along the interior highlands and Blue Ridge and foothills, dry days occur least frequently (<40%).

Days with very light and light precipitation are the second most frequent during the summer time. Very light precipitation occurs on nearly 20% of days

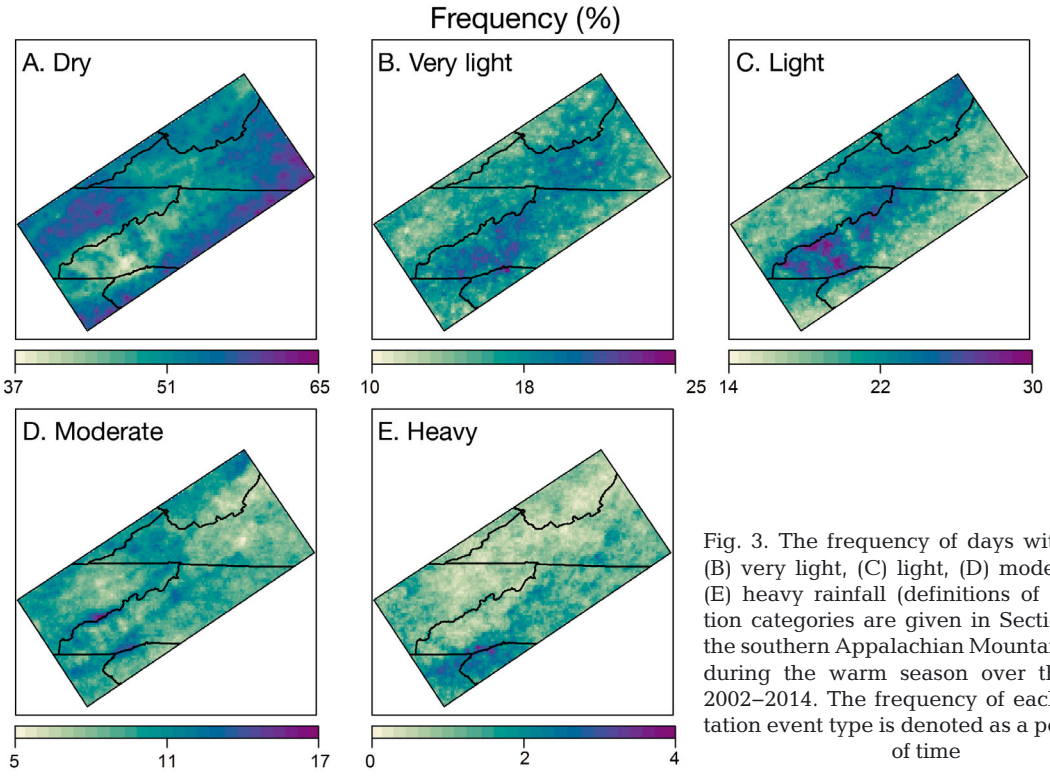

Fig. 3. The frequency of days with (A) no, (B) very light, (C) light, (D) moderate, and (E) heavy rainfall (definitions of precipitation categories are given in Section 2.4) in the southern Appalachian Mountains (SAM) during the warm season over the period 2002–2014. The frequency of each precipitation event type is denoted as a percentage of time

across the interior highlands and up to 25% of days on the most exposed areas of the southern Blue Ridge and foothills. Light precipitation is also more frequent throughout these regions. It occurs on up to 30% of days in the interior highlands and southern Blue Ridge and foothills regions. These 2 precipitation event types collectively account for more than half of the summer precipitation climatology across the high elevation areas of the SAM. Very light and light precipitation occur least frequently (e.g. <15%) throughout the intervening valleys and across the Piedmont.

Days with moderate or heavy precipitation occur least frequently across the SAM, although several topographic gradients are present. The maximum frequency of moderate precipitation occurs along the western slopes of the interior highlands, where it develops on up to 17% of the days. Moderate precipitation frequencies decrease in the adjacent intervening valleys to <6%. However, it occurs more frequently (e.g. 11%) along the northwest slopes and plateau, and across the Blue Ridge and foothills. Heavy precipitation events occur on <1% of days along the northwestern slopes and plateau and in northwestern parts of the interior highlands and intervening valleys. In contrast, it occurs on up to 4% of days along the southern Blue Ridge and foothills region and 2% of days in places throughout the Piedmont.

There is a wide range of circulation patterns that are linked with the occurrence of each precipitation event type across the different physiographic regions of the SAM. In general, each of the precipitation event types occurs with the greatest frequency in the left and lower left sections of the SOM space, which correspond with middle tropospheric southwesterly flow over the SAM. Moreover, precipitation events in this section of the SOM most frequently occur in the interior highlands, along the Blue Ridge and foothills, and least frequently in the intervening valleys and the Piedmont. Mean summer precipitation is also greatest in these locations throughout this section of the SOM (Fig. 4). The precipitation event types occur with the least frequency in the right and upper right sections of the SOM space, which correspond with northwesterly flow over the SAM. Precipitation events in this section of the SOM most frequently occur in the interior highlands and least frequently across the remaining portions of the SAM, including the northwest slopes and plateau, intervening valleys, Blue Ridge and foothills, and the Piedmont. Mean sum-

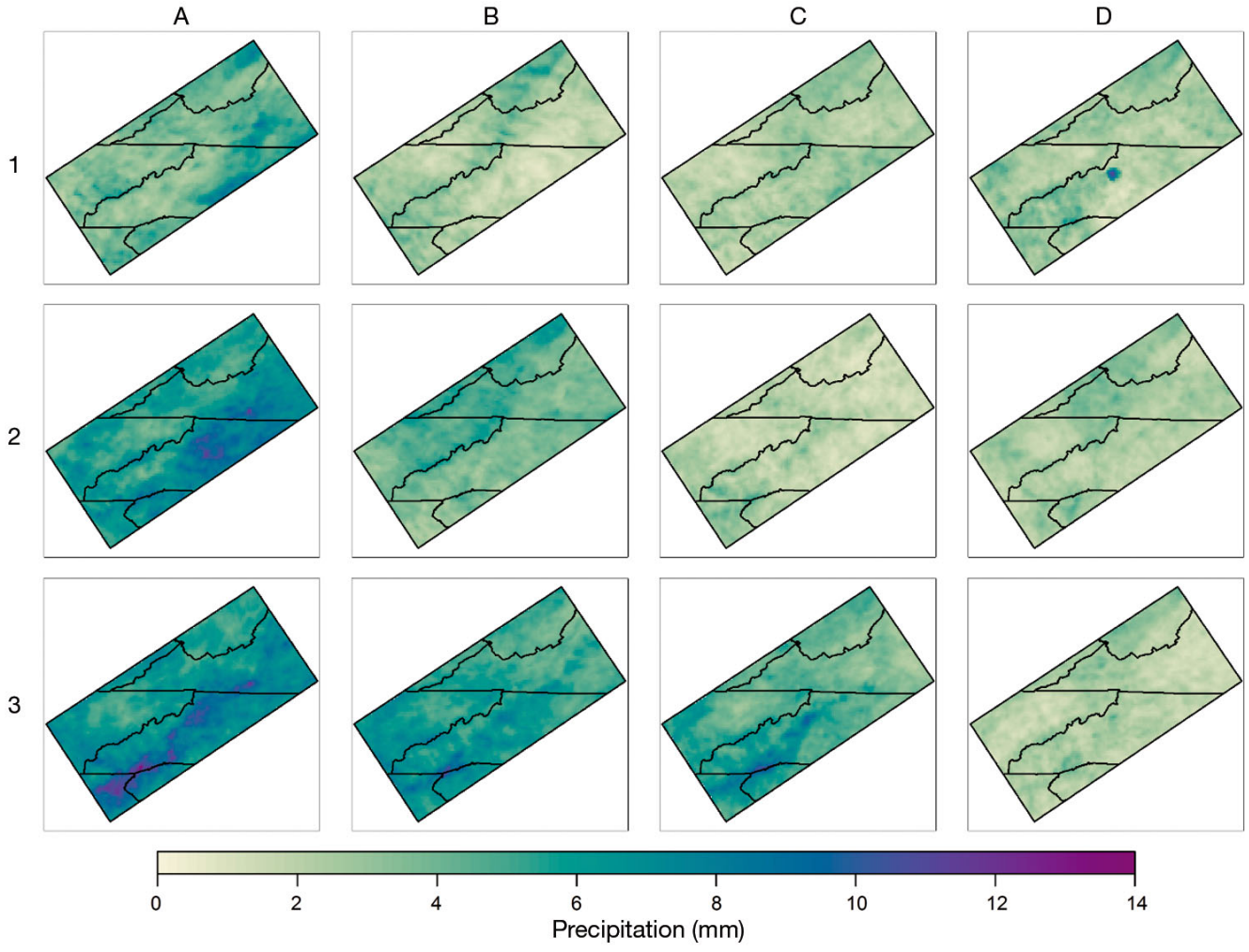

Fig. 4. The mean summer precipitation corresponding to the days in each node of the self-organizing map (SOM). In general, the most rainfall occurs in association with nodes in the lower left corner of the SOM, whereas the least rainfall occurs in the upper right portion of the SOM

mer precipitation is the lowest across these regions in this section of the SOM (Fig. 4).

Dry days occur with the greatest frequency in the right and upper right sections of the SOM space (Fig. 5), which correspond with northwesterly flow over the region (i.e. an upstream ridge and a downstream trough). They are especially common in the intervening valleys and Piedmont, occurring up to 90% of the time. Dry days are least frequent in the interior highlands, northwest slopes and plateau, and along the Blue Ridge and foothills, especially for the circulation patterns in the left and lower left sections of the SOM space corresponding to southwesterly flow over the SAM. Here, dry days occur most frequently (30–40% of the time) in the intervening valleys and Piedmont, and least frequently (10–20% of the time) across the interior highlands, northwest slopes and plateau, and along the Blue Ridge and foothills.

The patterns of very light rainfall are different compared to those with no precipitation (Fig. 6). In general, very light rainfall does not show as marked variations in frequency across the SOM, relative to the other event types. This indicates that it is associated with a wide range of circulation patterns during the summer. However, there are some notable variations in the pattern across the physiographic regions. First, very light rainfall occurs most frequently on 20–50% of days throughout the interior highlands and along the Blue Ridge and foothills. It occurs with the least frequency (<20% of the time) across the lower elevations, including places in the intervening valleys, the Piedmont, and various smaller valleys that bisect the interior highlands.

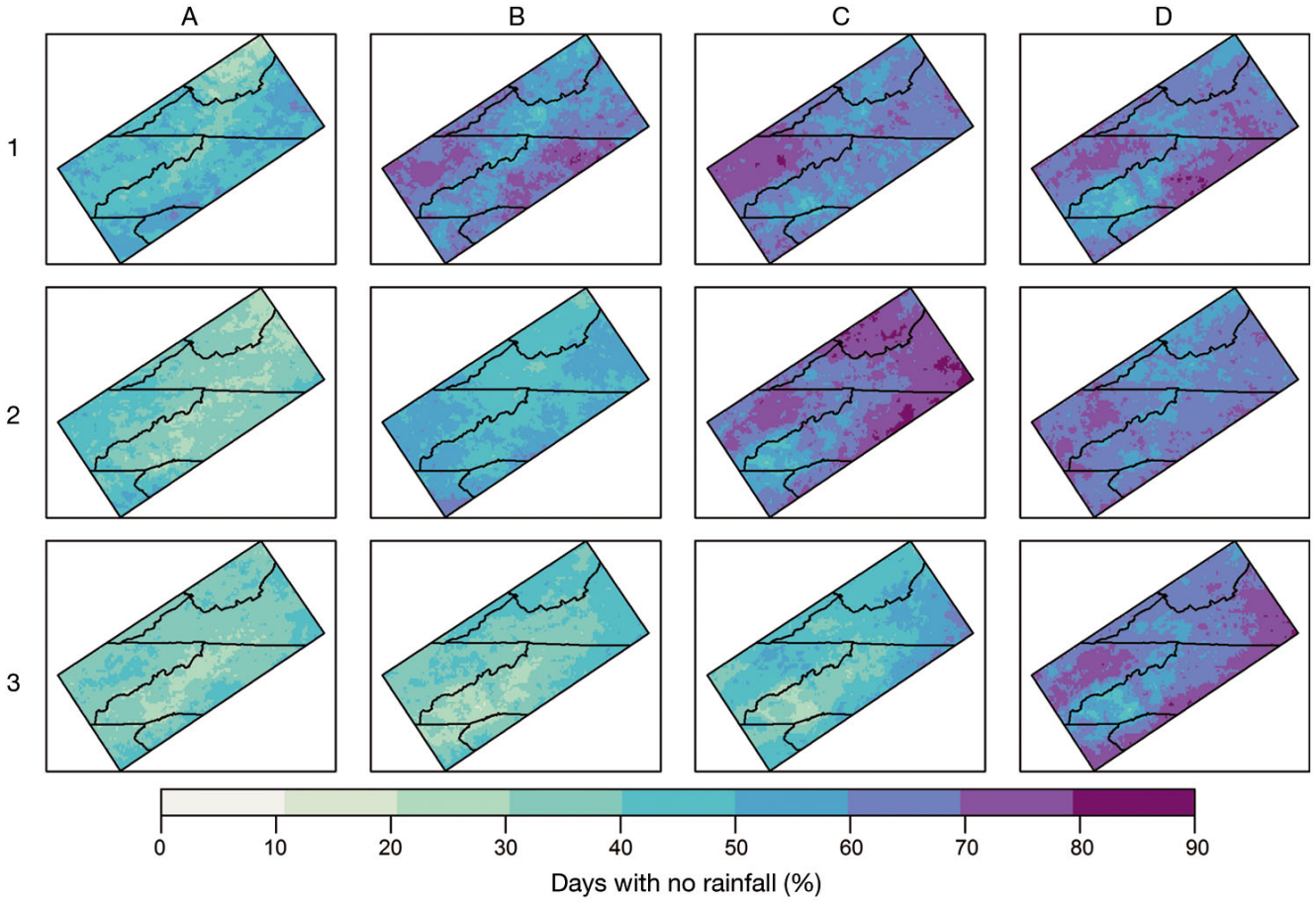

Fig. 5. Days with no rainfall are plotted in the self-organizing map based on their occurrence as a percentage of time when the associated circulation patterns are present from node to node

Light rainfall occurs with the greatest frequency along the left and lower left sections of the SOM, which correspond to southwesterly flow (trough upstream) and westerly flow (trough overhead) (Fig. 7). Light rainfall in this section of the SOM occurs most frequently (30–60% of the time) in the northwestern slopes and plateaus, the interior highlands, and along the Blue Ridge and foothills. Light rainfall occurs with the least frequency, <30% of the time, in the intervening valleys and the Piedmont. In the upper right part of the SOM, light rainfall occurs with the least frequency in connection with northwesterly to west northwesterly flow (i.e. ridge upstream or over the region). Days with light rainfall in this part of the SOM occur with the greatest frequency (20–30% of the time) throughout the interior highlands and some isolated areas of the northwest slopes and plateaus and southern Blue Ridge and foothills. They are least frequent in the intervening valleys and the Piedmont, occurring <20% of the time.

Moderate rainfall events are strongly tied to southwesterly flow patterns as revealed by the higher percentages of occurrence in the lower left section of the SOM (Fig. 8). Within this section, moderate rainfall occurs most frequently (20–40% of the time) in the Piedmont and parts of the Blue Ridge and foothills along the North Carolina–Virginia border. It occurs least frequently (10–20% of the time) throughout the interior highlands, intervening valleys, and the northwestern slopes and plateaus. Moderate rainfall events occur least frequently in association with the patterns of northwesterly flow found in the middle to upper right section of the SOM space. It was most frequent (10–20% of the time) along some of the northwestern slopes and plateaus and in a few places in the interior highlands. It was least frequent (<10% of the time) in the remaining regions of the SAM, including the intervening valleys, the Blue Ridge and foothills, and the Piedmont.

Heavy precipitation is the least frequently occurring precipitation event type across the SAM, and is

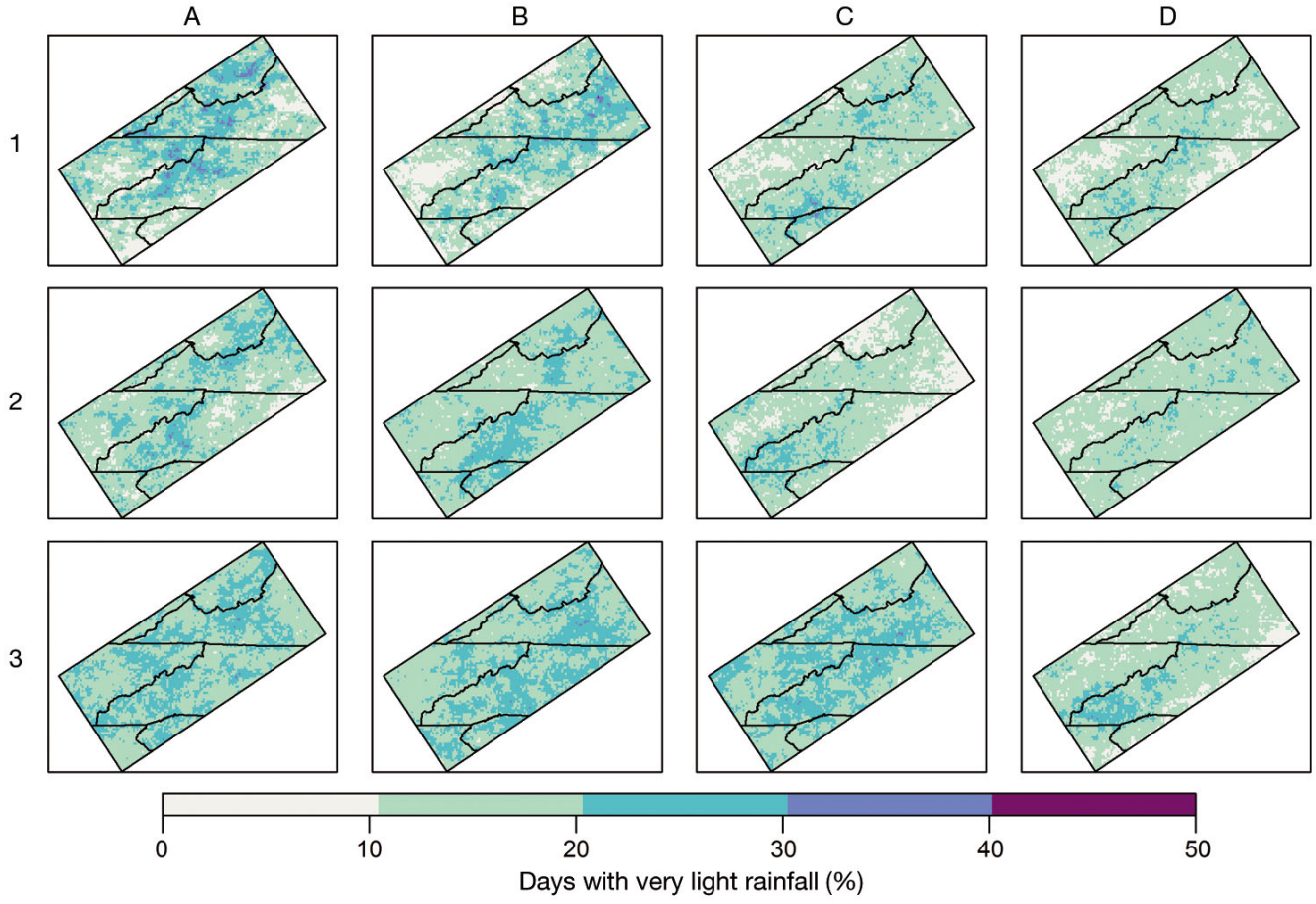

Fig. 6. Days with very light rainfall are plotted in the self-organizing map based on their occurrence as a percentage of time when the associated circulation patterns are present from node to node

connected with a subset of the circulation patterns in the lower left section of the SOM, which display a west southwesterly to southwesterly flow (i.e. trough immediately upstream) (Fig. 9). In this area of the SOM, heavy rainfall occurs up to 16% of the time along the Blue Ridge and foothills of Virginia, and 4–12% of the time in the Piedmont and the southern Blue Ridge and foothills of North Carolina. Heavy rainfall also occurs 4–12% of the time across the Blue Ridge and foothills in connection with southwesterly to southerly flow. It is a rare occurrence in the remaining sections of the SOM (<4% of the time).

4. DISCUSSION

This study examined the relationships between summer atmospheric circulation patterns and the occurrence of precipitation across different physiographic regions of the SAM. We used a SOM to categorize daily circulation patterns across the SEUS from daily geopotential height data. The SOM is a type of artificial neural network that allows the user to classify, spatially organize, and visualize the commonalities and differences between circulation patterns. Five precipitation event types were identified from daily PRISM data on a 4 × 4 km grid over the SAM and associated with the circulation types identified in the SOM.

Middle tropospheric ridging patterns were present on a majority (56%) of days during the summer season study period (e.g. right and upper right sections of the SOM) with middle tropospheric northwesterly flow over the SAM (Fig. 10). However, there were variations in these circulation types corresponding to differences in the strength and positioning of the ridge. Precipitation frequencies were the lowest on days displaying these ridging patterns, and, in many of these patterns, this may be tied to the presence of subsidence in the middle troposphere downstream of the ridge axis and high levels of stability from inversions or stable layers that cap daytime convection.

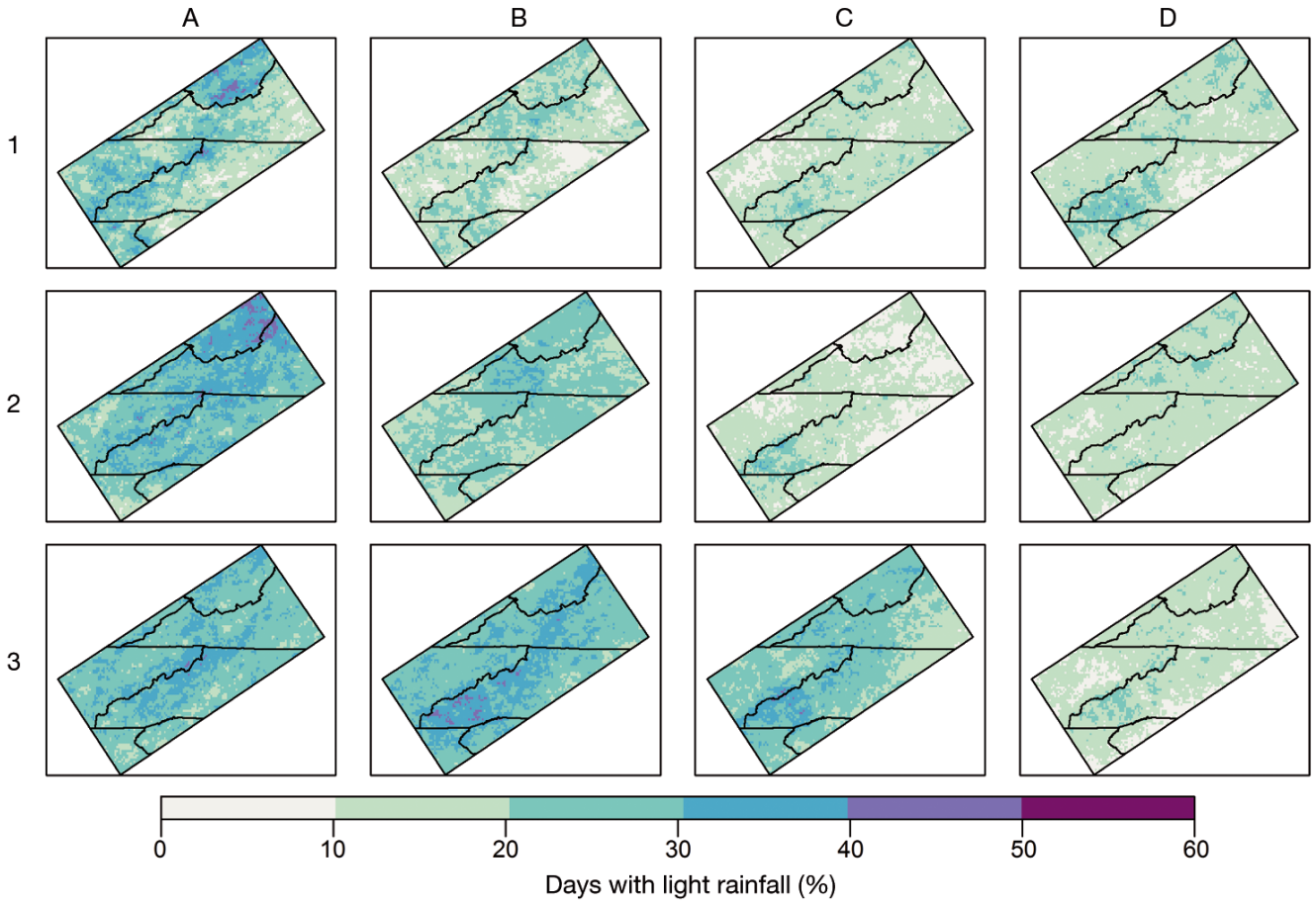

Fig. 7. Days with light rainfall are plotted in the self-organizing map based on their occurrence as a percentage of time when the associated circulation patterns are present from node to node

Composites of the surface circulation pattern revealed 2 distinct patterns: (1) an area of lower MSLP located to the northeast as a 500 mb ridge builds in from the west (i.e. B1, C1, and B2), and (2) a stacked ridging pattern tied to the presence of the NASH (i.e. remaining 500 mb ridging patterns). In spite of the drier, more stable conditions in the lower troposphere, very light or light rainfall occurred on 40–60% of the days over the higher terrain along the interior highlands and a few areas of the southern Blue Ridge and foothills region. This precipitation is usually associated with deep convection over the elevated terrain. In contrast, dry conditions occurred 70–90% of the time in the lower lying regions, including the Piedmont and intervening valleys.

The duration of middle tropospheric ridging (i.e. westward displaced NASH) is associated with reduced air quality (Diem et al. 2010), soil moisture deficits (Doublin & Grundstein 2008), and drought (Ortegren et al. 2011) across the SEUS. Several of the ridging patterns in this section of the SOM were persistent, with many instances where ridging occurred over the SAM for a period of several days or more. So while the occurrence of 500 mb ridging patterns promote dryness on a synoptic scale, localized convection over the mountains produces precipitation that keeps these mountainous areas relatively wet on many of these days (Figs. 5–7). This result is consistent with Wilson & Barros (2014), who identified that light rainfall events accounted for up to 50% of the annual accumulation across a small transect of high elevations in western North Carolina. These results suggest that these mountainous areas are thereby potentially buffered from extended dry periods and drought, which develop during periods of persistent ridging patterns across the SEUS (Seager et al. 2009, Kam et al. 2014).

The remaining 5 nodes in the left and lower left sections of the SOM occurred on 44% of the days during the summer season study period and were associated with an upstream trough or trough overhead with southwest or westerly flow, respectively

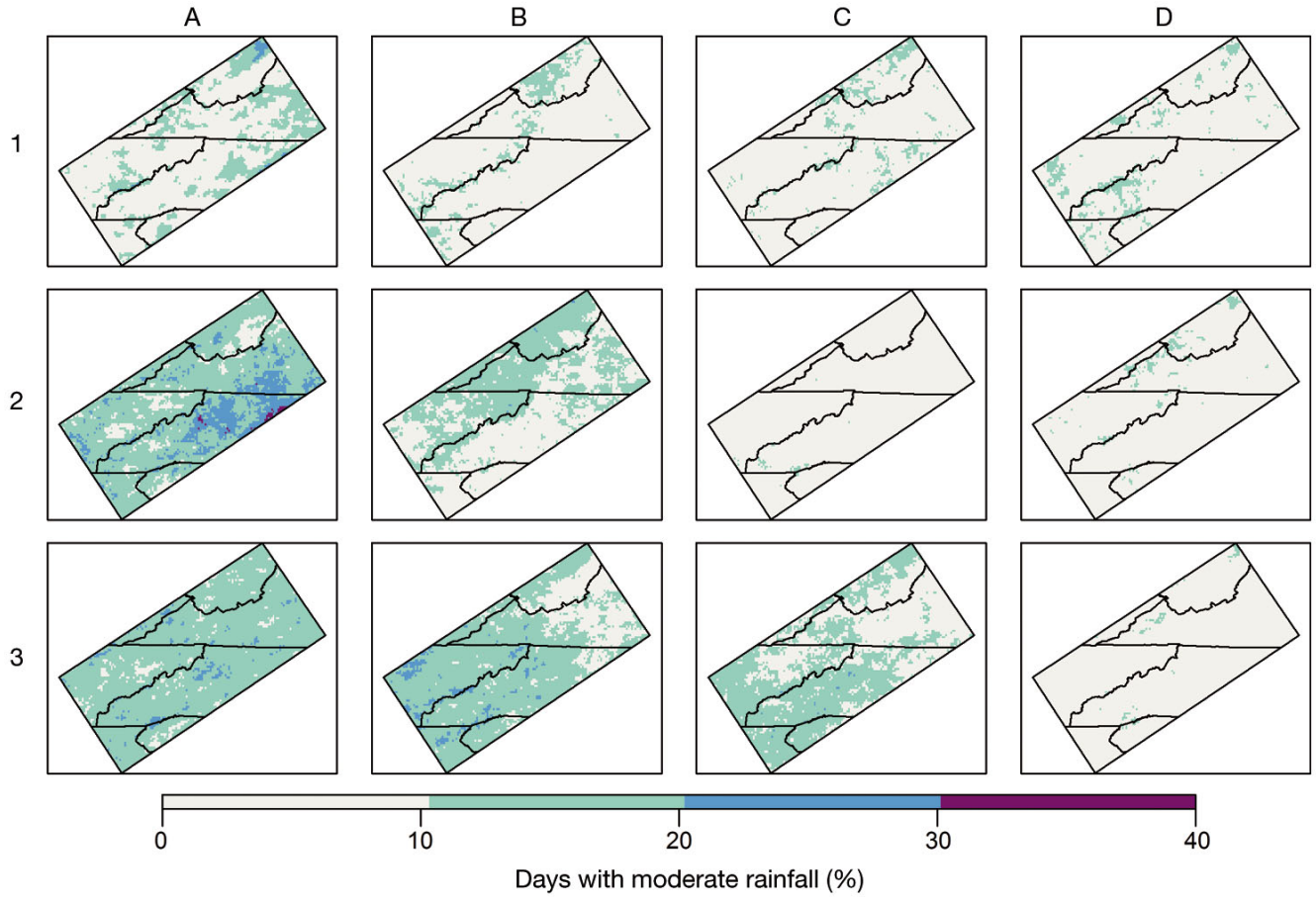

Fig. 8. Days with moderate rainfall are plotted in the self-organizing map based on their occurrence as a percentage of time when the associated circulation patterns are present from node to node

(Fig. 10). There were variations in these circulation types corresponding to differences in the strength and positioning of the upstream trough and downstream ridge. Composites of the surface circulation patterns revealed moist southerly flow over the SEUS as a surface front approached the region and the NASH retreated towards the southeast. As in Konrad (1996), precipitation frequencies were the greatest on days displaying these patterns, especially moderate and heavy events. This may be tied to increased instability (e.g. greater convective available potential energy) from low-level moisture advection out of the Gulf of Mexico and middle tropospheric cooling with the approach of a 500 mb trough. Previous studies (Keim 1996, Kelly et al. 2012) also highlighted the importance of frontal boundaries in producing heavy precipitation across the region. This section of the SOM also included the most persistent circulation pattern, with a deep 500 mb trough located immediately downstream of the SAM. Although this pattern occurred least frequently overall, its duration tended to be the longest. Very light and light rainfall occurred 50–70% of the time in the interior highlands, Blue Ridge and foothills, and local portions of the northwestern slopes and plateaus, and <30% of the time in the intervening valleys and the Piedmont. Moderate and heavy rainfall events were also most frequent (20–40% and <20% of the time, respectively) in the North Carolina–Virginia Piedmont and exposed locations along the southern Blue Ridge and foothills region. While some of the troughing patterns are uncommon during the summer, they can produce substantial precipitation when they do occur.

The ability to forecast future climate shifts depends on the ability of the models to reproduce the position of mid-latitude ridges and troughs, as well as their frequency of occurrence (Pastor & Casado 2012). Much research has utilized the SOM technique to perform this evaluation. While the SOM itself is not feasible for use in operational forecasting, it does provide a source of guidance that improves the process of providing conditional probabilities of differ-

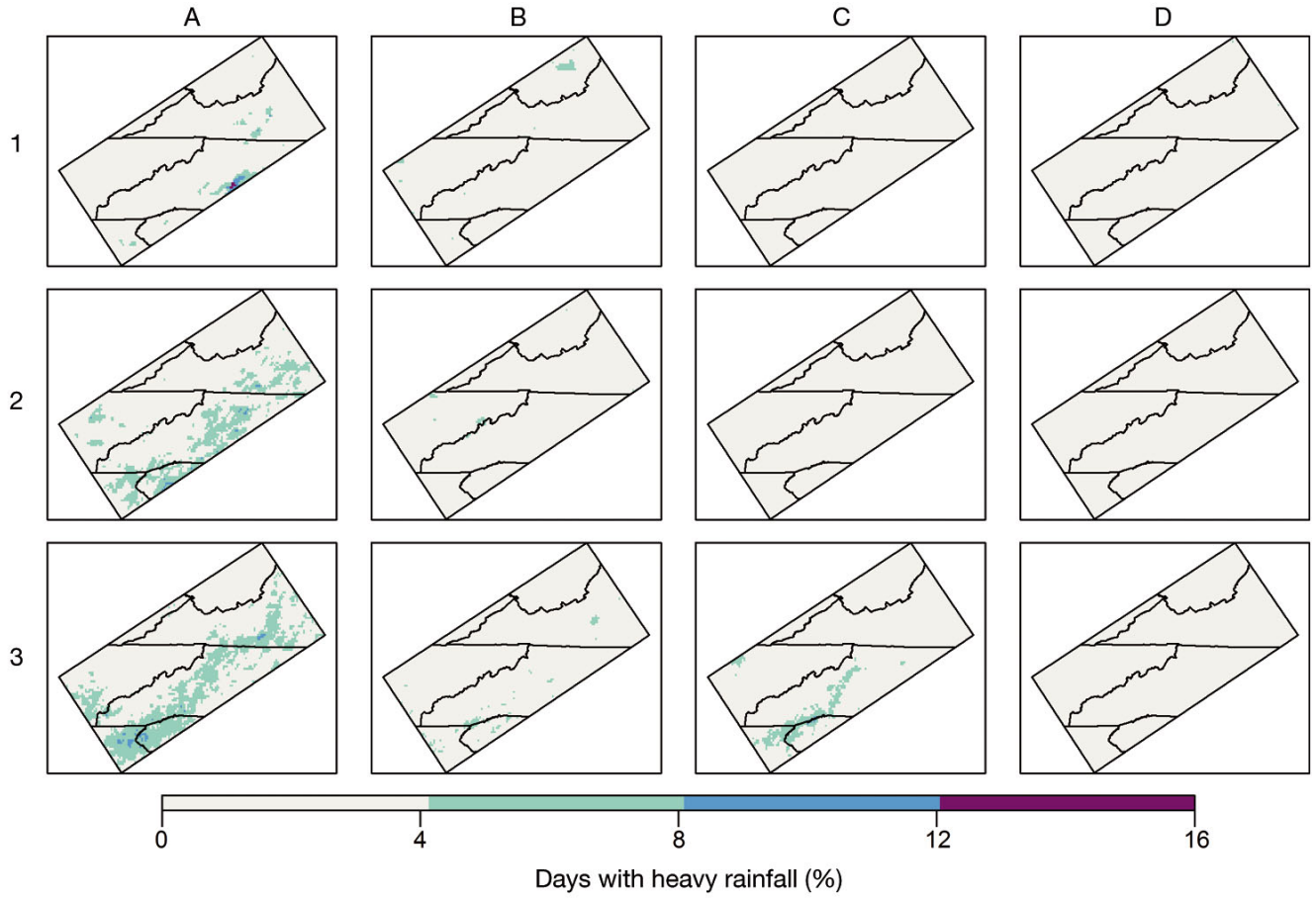

Fig. 9. Days with heavy rainfall are plotted in the self-organizing map based on their occurrence as a percentage of time when the associated circulation patterns are present from node to node

ent circulation types (Nowotarski & Jensen 2013). This research shows areas within the SAM that most and least frequently receive different types of daily precipitation events, and how the observed synoptic circulation patterns during the summer affect these frequencies. Subtle shifts in the frequency of different circulation patterns will influence the spatial distribution of precipitation from node to node.

Most of the research using SOMs in synoptic climatology has focused on a similar evaluation of these circulation changes and their influence on other variables, such as precipitation. However, the technique also provides a valuable tool for a comprehensive evaluation of the climate models themselves (Gibson et al. 2016b). Future work is therefore needed not only to identify how synoptic patterns across the SEUS are changing in a changing climate, but also to provide a climate model evaluation of the relationships between circulation and precipitation. This is especially important for the SAM region, as it provides a range of ecosystem services and serves as a water tower for rapidly growing population centers across the SEUS.

LITERATURE CITED

Barry RG (2008) Mountain weather and climate, 3rd edn. Cambridge University Press, Cambridge

Basist A, Bell GD, Meentemeyer V (1994) Statistical relationships between topography and precipitation patterns. J Clim 7:1305–1315

Berrisford P, Dee DPKF, Fielding K, Fuentes M, Kallberg P, Kobayashi S, Uppala S (2009) The ERA-interim archive. ERA report series (1), European Centre for Medium Range Weather Forecasts, Reading

Bhatt BC, Nakamura K (2005) Characteristics of monsoon rainfall around the Himalayas revealed by TRMM precipitation radar. Mon Weather Rev 133:149–165

Bruijnzeel LA, Mulligan M, Scatena FN (2011) Hydrometeorology of tropical montane cloud forests: emerging patterns. Hydrol Processes 25:465–498

Caruso NM, Sears MW, Adams DC, Lips KR (2014) Widespread rapid reductions in body size of adult salamanders in response to climate change. Glob Change Biol 20: 1751–1759

Christensen JH, Kumar KK, Aldrian E, An S-I and others (2013) Climate phenomena and their relevance for future regional climate change. In Stocker TF, Qin D, Plattner GK, Tignor M and others (eds) Climate change 2013: the physical science basis. Contribution of Working Group I to the Fifth Assessment Report of the Intergovernmental

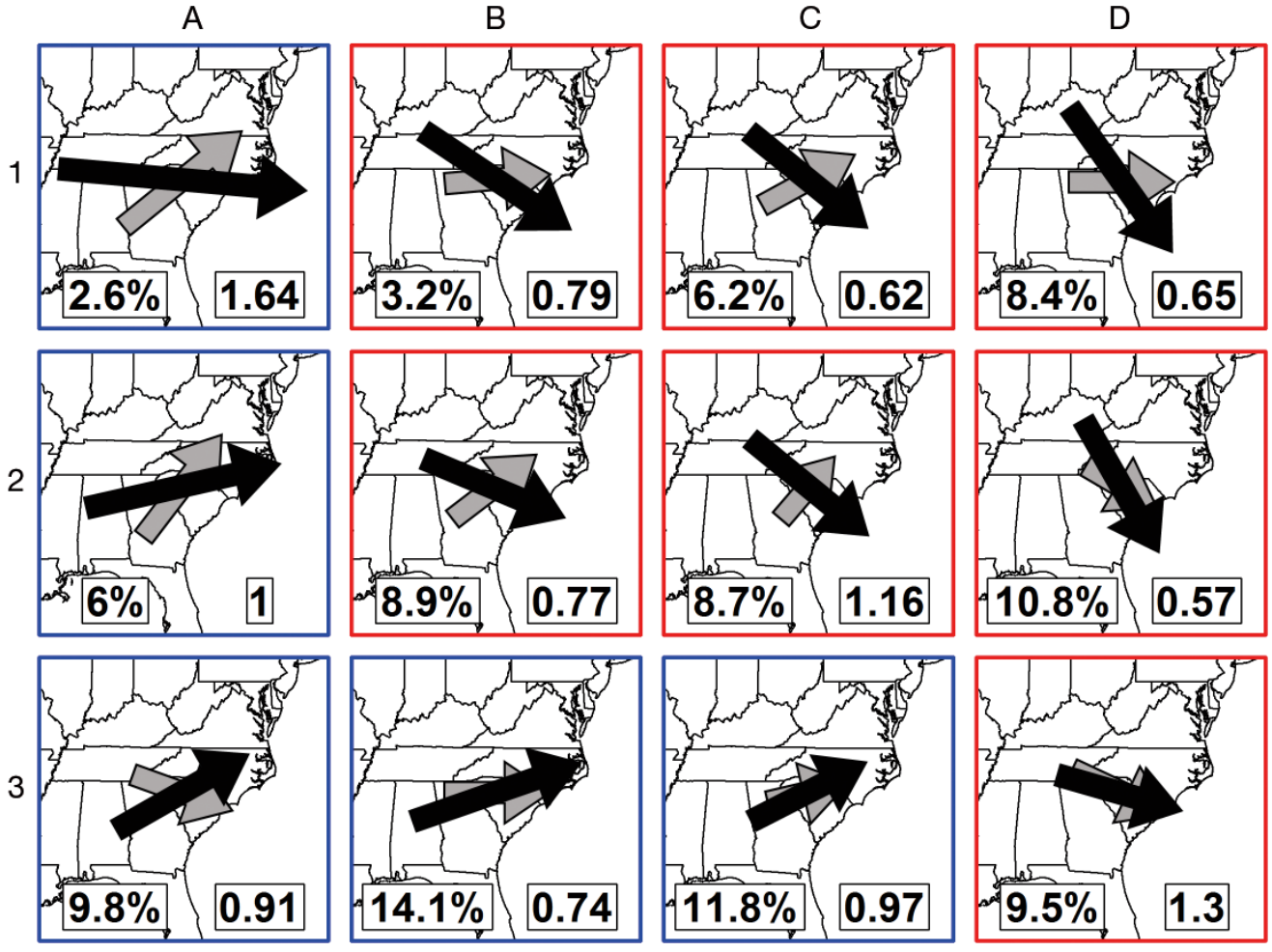

Fig. 10. Summary of the results found in this study using the self-organizing map. Primary wind direction is plotted based on the 500 mb level (black arrows) and the 850 mb level (grey arrows) over the southern Appalachian Mountains. Arrow length depicts the magnitude. Nodes outlined in red are associated with varying degrees of northwest flow and lower precipitation frequencies, while nodes outlined in blue are associated with southwest flow and higher precipitation frequencies. Values at bottom of panels as in Fig. 2

Panel on Climate Change. Cambridge University Press, Cambridge

Daly C, Neilson RP, Phillips DL (1994) A statistical-topographic model for mapping climatological precipitation over mountainous terrain. J Appl Meteorol 33:140–158

Daly C, Halbleib M, Smith JI, Gibson WP, Doggett MK, Taylor GH, Pasteris PP (2008) Physiographically sensitive mapping of climatological temperature and precipitation across the conterminous United States. Int J Climatol 28: 2031–2064

de Jong C, Lawler D, Essery R (2009) Mountain hydroclimatology and snow seasonality — perspectives on climate impacts, snow seasonality and hydrological change in mountain environments. Hydrol Processes 23:955–961

Dee DP, Uppala SM, Simmons AJ, Berrisford P and others (2011) The ERA-Interim reanalysis: configuration and performance of the data assimilation system. QJR Meteorol Soc 137:553–597

Diem JE (2006) Synoptic-scale controls of summer precipitation in the Southeastern United States. J Clim 19: 613–621

Diem JE (2013) Influences of the Bermuda High and atmospheric moistening on changes in summer rainfall in the Atlanta, Georgia region, the United States. Int J Climatol 33:160–172

Diem JE, Hursey MA, Morris IR, Murray AC, Rodriguez RA (2010) Upper-level atmospheric circulation patterns and ground-level ozone in the Atlanta metropolitan area. J Appl Meteorol Climatol 49:2185–2196

Doswell CA, Brooks HE, Maddox RA (1996) Flash flood forecasting : an ingredients-based methodology. Weather Forecast 11:560–581

Doublin JK, Grundstein AJ (2008) Warm-season soil-moisture deficits in the Southern United States. Phys Geogr 29:3–18

Gibson PB, Perkins-Kirkpatrick SE, Renwick JA (2016a) Projected changes in synoptic weather patterns over New Zealand examined through self-organizing maps. Int J Climatol 36:3934–3948

Gibson PB, Uotila P, Perkins-Kirkpatrick SE, Alexander LV, Pitman AJ (2016b) Evaluating synoptic systems in the CMIP5 climate models over the Australian region. Clim Dyn 47:2235–2251

Hartmann DJ, Klein Tank AMG, Rusticucci M, Alexander LV

and others (2013) Observations: atmosphere and surface. In Stocker TF, Qin D, Plattner GK, Tignor M and others (eds) Climate Change 2013: the physical science basis. Contribution of Working Group I to the Fifth Assessment Report of the Intergovernmental Panel on Climate Change. Cambridge University Press, Cambridge

Hewitson BC, Crane RG (2002) Self-organizing maps: applications to synoptic climatology. Clim Res 22:13–26

Horton DE, Johnson NC, Singh D, Swain DL, Rajaratnam B, Diffenbaugh NS (2015) Contribution of changes in atmospheric circulation patterns to extreme temperature trends. Nature 522:465–469

Huva R, Dargaville R, Rayner P (2015) The impact of filtering self-organizing maps: a case study with Australian pressure and rainfall. Int J Climatol 35:624–633

Kam J, Sheffield J, Wood EF (2014) A multiscale analysis of drought and pluvial mechanisms for the Southeastern United States. J Geophys Res D Atmos 119:7348–7367

Keim B (1996) Spatial, synoptic, and seasonal patterns of heavy rainfall in the southeastern United States. Phys Geogr 17:313–328

Kelly GM, Perry LB, Taubman BF, Soulé PT (2012) Synoptic classification of 2009–2010 precipitation events in the southern Appalachian Mountains, USA. Clim Res 55:1–15

Kohonen T (1997) Self-organizing maps, 3rd edn. Springer-Verlag, New York, NY

Konrad CE (1996) Relationships between precipitation event types and topography in the Southern Blue Ridge Mountains of the Southeastern USA. Int J Climatol 16:49–62

Konrad CE (1997) Synoptic-scale features associated with warm season heavy rainfall over the interior Southeastern United States. Weather Forecast 12:557–571

Konrad CE (2001) The most extreme precipitation events over the Eastern United States from 1950 to 1996: considerations of scale. J Hydrometeorol 2:309–325

Kramer RA, Eisen-Hecht JI (2002) Estimating the economic value of water quality protection in the Catawba River basin. Water Resour Res 38(9):1182

Labosier CF, Quiring SM (2013) Hydroclimatology of the Southeastern USA. Clim Res 57:157–171

Li W, Li L, Fu R, Deng Y, Wang H (2011) Changes to the North Atlantic Subtropical High and its role in the intensification of summer rainfall variability in the Southeastern United States. J Clim 24:1499–1506

Li L, Li W, Kushnir Y (2012) Variation of the North Atlantic subtropical high western ridge and its implication to Southeastern US summer precipitation. Clim Dyn 39: 1401–1412

Lin YL, Chiao S, Wang TA, Kaplan ML, Weglarz RP (2001) Some common ingredients for heavy orographic rainfall. Weather Forecast 16:633–661

Lynch A, Uotila P, Cassano JJ (2006) Changes in synoptic weather patterns in the polar regions in the twentieth and twenty-first centuries. 2. Antarctic. Int J Climatol 26: 1181–1199

Maddox RA, Chappell CF, Hoxit LR (1979) Synoptic and meso-α scale aspects of flash flood events. Bull Am Meteorol Soc 60:115–123

Messerli B, Viviroli D, Weingartner R (2004) Mountains of the world: vulnerable water towers for the 21st century. Ambio 13:29–34

Negley TL, Eshleman KN (2006) Comparison of stormflow responses of surface-mined and forested watersheds in the Appalachian Mountains, USA. Hydrol Processes 20: 3467–3483

Nowotarski CJ, Jensen AA (2013) Classifying proximity soundings with self-organizing maps toward improving supercell and tornado forecasting. Weather Forecast 28: 783–801

Ortegren JT, Knapp PA, Maxwell JT, Tyminski WP, Soulé PT (2011) Ocean–atmosphere influences on low-frequency warm-season drought variability in the Gulf Coast and Southeastern United States. J Appl Meteorol Climatol 50:1177–1186

Parker MD, Ahijevych DA (2007) Convective episodes in the east-central United States. Mon Weather Rev 135: 3707–3727

Pastor MA, Casado MJ (2012) Use of circulation types classifications to evaluate AR4 climate models over the Euro-Atlantic region. Clim Dyn 39:2059–2077

Prat OP, Barros AP (2010) Assessing satellite-based precipitation estimates in the Southern Appalachian mountains using rain gauges and TRMM PR. Adv Geosci 25:143–153

Prism Climate Group (2015) Prism gridded climate data. Terms of use. http://prism.oregonstate.edu

Reinhardt K, Smith WK (2008) Leaf gas exchange of understory spruce-fir saplings in relict cloud forests, southern Appalachian Mountains, USA. Tree Physiol 28:113–122

Rickenbach TM, Nieto-Ferreira R, Zarzar C, Nelson B (2015) A seasonal and diurnal climatology of precipitation organization in the southeastern United States. Quart J R Meteorol Soc 141:1938–1956

Ruhl JB (2005) Water wars, Eastern style: divvying up the Apalachicola-Chattahoochee-Flint River Basin. J Contemp Water Res Educ 131:47–54

Seager R, Tzanova A, Nakamura J (2009) Drought in the southeastern United States: causes, variability over the last millennium, and the potential for future hydroclimate change. J Clim 22:5021–5045

Sheridan SC, Lee CC (2011) The self-organizing map in synoptic climatological research. Prog Phys Geogr 35:109–119

Skific N, Francis J (2012) Self-organizing maps: a powerful tool for the atmospheric sciences. In: Johnsson M (ed) Applications of self-organizing maps. InTech, Rijeka

Viviroli D, Dürr HH, Messerli B, Meybeck M, Weingartner R (2007) Mountains of the world, water towers for humanity: typology, mapping, and global significance. Water Resour Res 43:1–13

Wang H, Fu R, Kumar A, Li W (2010) Intensification of summer rainfall variability in the Southeastern United States during recent decades. J Hydrometeorol 11:1007–1018

Wehrens R, Buydens LMC (2007) Self- and super-organising map in R: the Kohonen package. J Stat Softw 21:1–19

Wilson AM, Barros AP (2014) An investigation of warm rainfall microphysics in the Southern Appalachians: orographic enhancement via low-level seeder–feeder interactions. J Atmos Sci 71:1783–1805

Wise EK, Dannenberg MP (2014) Persistence of pressure patterns over North America and the North Pacific since AD 1500. Nat Commun 5:4912

Yang J, Gong DY (2010) Intensified reduction in summertime light rainfall over mountains compared with plains in Eastern China: a letter. Clim Change 100:807–815

Yarnal B, Comrie AC, Frakes B, Brown DP (2001) Developments and prospects in synoptic climatology. Int J Climatol 21:1923–1950

Zhang J, Howard K, Langston C, Vasiloff S and others (2011) National Mosaic and Multi-Sensor QPE (NMQ) System: description, results, and future plans. Bull Am Meteorol Soc 92:1321–1338

Editorial responsibility: Balaji Rajagopalan, Boulder, Colorado, USA

Submitted: November 22, 2017; Accepted: September 28, 2017
Proofs received from author(s): December 13, 2017